Free Radical Biology and Medicine 130 (2019) 163–173

Contents lists available at ScienceDirect

Free Radical Biology and Medicine

journal homepage: www.elsevier.com/locate/freeradbiomed

Original article

Cancer-associated fibroblasts modify lung cancer metabolism involving ROS and TGF-β signaling

Alberto Cruz-Bermúdez[a,*], Raquel Laza-Briviesca[a,1], Ramiro J. Vicente-Blanco[a,1], Aránzazu García-Grande[b], Maria José Coronado[c], Sara Laine-Menéndez[d], Cristina Alfaro[a], Juan Cristobal Sanchez[a], Fernando Franco[a], Virginia Calvo[a], Atocha Romero[a], Paloma Martin-Acosta[e,f], Clara Salas[e], José Miguel Garcia[a], Mariano Provencio[a,*]

[a] Servicio de Oncología Médica, Instituto de Investigación Sanitaria Puerta de Hierro-Segovia de Arana (IDIPHISA), Hospital Universitario Puerta de Hierro-Majadahonda, Madrid, Spain
[b] Flow Cytometry Core Facility, Hospital Universitario Puerta de Hierro Majadahonda Calle, Madrid, Spain
[c] Confocal Microscopy Core Facility, Hospital Universitario Puerta de Hierro Majadahonda, Madrid, Spain
[d] Mitochondrial and neuromuscular disease laboratory, Instituto de Investigación Hospital "12 de Octubre" (i+12), Madrid, Spain
[e] Departamento de Patología, Hospital Universitario Puerta de Hierro-Majadahonda, Madrid, Spain
[f] Centro de Investigación Biomédica en Red de Cáncer (CIBERONC), Madrid, Spain

ARTICLE INFO

Keywords:
Cancer
Metabolism
Reverse Warburg effect
Cancer associated fibroblasts mitochondria
OXPHOS

ABSTRACT

Lung cancer is a major public health problem due to its high incidence and mortality rate. The altered metabolism in lung cancer is key for the diagnosis and has implications on both, the prognosis and the response to treatments. Although Cancer-associated fibroblasts (CAFs) are one of the major components of the tumor microenvironment, little is known about their role in lung cancer metabolism.

We studied tumor biopsies from a cohort of 12 stage IIIA lung adenocarcinoma patients and saw a positive correlation between the grade of fibrosis and the glycolysis phenotype (Low PGC-1α and High GAPDH/MT-CO1 ratio mRNA levels). These results were confirmed and extended to other metabolism-related genes through the *in silico* data analysis from 73 stage IIIA lung adenocarcinoma patients available in TCGA. Interestingly, these relationships are not observed with the CAFs marker α-SMA in both cohorts.

To characterize the mechanism, *in vitro* co-culture studies were carried out using two NSCLC cell lines (A549 and H1299 cells) and two different fibroblast cell lines. Our results confirm that a metabolic reprogramming involving ROS and TGF-β signaling occurs in lung cancer cells and fibroblasts independently of α-SMA induction. Under co-culture conditions, Cancer-Associated fibroblasts increase their glycolytic ability. On the other hand, tumor cells increase their mitochondrial function. Moreover, the differential capability among tumor cells to induce this metabolic shift and also the role of the basal fibroblasts Oxphos Phosphorylation (OXPHOS) function modifying this phenomenon could have implications on both, the diagnosis and prognosis of patients. Further knowledge in the mechanism involved may allow the development of new therapies.

1. Introduction

One of the tumor cell´s hallmarks is its altered metabolism, adapted to support a rapid cell growth [1]. This, from a basic standpoint, is achieved by an increase in aerobic glycolysis, known as the Warburg effect, which allows the contribution of intermediary metabolites used in anabolic processes [2,3]. In fact, one of the most important systems for cancer diagnosis, positron emission tomography with the radiopharmaceutical 18-Fluorodeoxyglucose (FDG-PET), is based on this singular metabolism of tumors, which forces them to consume more glucose than the surrounding tissues [4].

Despite the importance of this altered metabolism, there is a lack of molecular and functional studies that approximate to what is really happening *in vivo*. We know now that tumors are not uniform masses of

Abbreviations: OXPHOS, Oxidative phosphorylation; ROS, Reactive oxygen species; CAFs, Cancer associated fibroblasts; MIMP, Mitochondrial inner membrane potential

* Corresponding authors.
E-mail addresses: acruz@idiphim.org (A. Cruz-Bermúdez), mariano.provencio@salud.madrid.org (M. Provencio).
[1] These authors contributed equally.

https://doi.org/10.1016/j.freeradbiomed.2018.10.450
Received 21 August 2018; Received in revised form 22 October 2018; Accepted 30 October 2018
Available online 01 November 2018

cells. Besides the transformed cells, many cell types coexist, including fibroblasts, endothelial or immune cells, which results in what is known as tumor microenvironment. Following this line of thought, over the last years many studies focusing on the microenvironment have been conducted. This interest relies on the fact that different cell types communicate with each other, changing their behavior and thus conditioning tumor metabolism [5], tumor progression [6], and treatment response [7]. Therefore, additional studies on cancer metabolism are needed taking into account this complexity, since most studies have focused exclusively on analysis of isolated tumor cell lines. It is likely that the discrepancy between cancer basic knowledge and its clinical application is due to underestimation of the microenvironment component of tumors.

One of the most important components of the tumor microenvironment are the cancer associated fibroblasts (CAFs) [8], identified by the expression of proteins such as α-smooth muscle actin (α-SMA) and fibroblast activation protein (FAP) [9]. The role of CAFs at metabolic level has been recently described as the Reverse Warburg effect. According to this model, tumor cells within the microenvironment would activate the fibroblasts present by different factors and would control them, taking advantage of their metabolism. Although this phenomenon is still not completely understood, it seems to implicate a decrease on mitochondrial function in CAFs with the ensuing increase on glycolysis. This metabolic shift would lead to a release of highly energetic metabolic substrates to the microenvironment that would be used by the tumor cells through an increased OXPHOS function [10–13].

We have focused on lung cancer because it is a major public health problem. Lung cancer is the most common cancer worldwide in terms of incidence and it is also the leading cause of cancer-related death in the world despite new targeted therapies based on their mutational profile have been incorporated [14–16]. Approximately one-third of patients with non-small cell lung cancer (NSCLC) are diagnosed with locally advanced (stage III) disease. These patients experience poor overall survival due to the presence of metastatic diseases that are not adequately detected. Therefore, many patients are subjected to aggressive localized treatments, such as surgery or radiotherapy, when they already present advanced distant disease [17].

Usually lung tumors have a variable component of mesenchymal-parenchyma composed mainly of fibroblasts and collagen fibers [18]. Importantly, in spite of the clinical relevance of lung cancer (in which FDG-PET is a key diagnostic tool [19] and the fibroblasts are an important component of tumors [20]) the role of the microenvironment in metabolic reprogramming has not been studied.

Our results on stage IIIA NSCLC patients show a positive correlation between the grade of fibrosis and the glycolysis phenotype of the tumor. *In vitro* studies confirm that, a metabolic reprogramming involving ROS and TGF-β signaling occurs in lung cancer cells and fibroblasts independently of α-SMA induction and suggest that specific attributes among tumor cells and fibroblasts may modify or hamper this phenomenon.

2. Materials and methods

2.1. Patients

A cohort of 12 stage IIIA adenocarcinoma patients was studied. All studies were carried out using the Formalin-Fixed Paraffin Embedded tissue (FFPET) from diagnostic biopsies. All the experiments carried out in this study complied with current Spanish and European Union laws and the principles outlined in the Declaration of Helsinki. The study and experimental protocols were approved by the Hospital Universitario Puerta de Hierro Ethics Committee and written informed consent was obtained from all the patients recruited.

2.2. Fibrosis grade

The fibrosis grade was evaluated in the hematoxylin-eosin diagnostic slides at x50 magnification. A low (< 1/3 desmoplastic stroma) or high (> 1/3 desmoplastic stroma) score was assigned to each sample by three independent anatomical pathology technicians. Vimentin and cytokeratin immunostaining of tumor biopsies using specific antibodies were carried out to confirm the correct identification of tumor cells and fibroblasts on the hematoxylin-eosin samples.

2.3. RT-qPCR expression analysis

The RNA extraction from FFPET biopsies was performed using the “High Pure FFPET RNA isolation Kit” (Roche). The RNA from cells was extracted using the “RNeasy mini Kit with DNAse” (Qiagen) and the cDNA was synthetized using the “NZY First-Strand cDNA Synthesis Kit” (NZYtech).

PGC-1α, GAPDH, MT-CO1, LDHA, α-SMA, MCT4 and TGF-β mRNA expression was measured by qRT- PCR using the Taqman® gene expression assays Hs01016719_m1, Hs02758991_g1, Hs02596864_g1, Hs01378790_g1, Hs00426835_g1, Hs00358829_m1 and Hs00998133_m1 respectively. TBP (Hs00427621_m1) was used as endogenous control [21].

2.4. In silico analysis of TCGA patients

73 stage IIIA lung adenocarcinoma patients were analyzed using R2: Genomics Analysis and Visualization Platform (http://r2.amc.nl, dataset id “Tumor lung adenocarcinoma – TCGA – 515 –rsem-tcgars“).

2.5. Cell lines

A549 and H1299 were obtained from the ATCC, Control Fibroblasts 1, 2 and 3 (CF1, CF2, CF3) were primary cultures derived from healthy donors and the Affected Fibroblast (AF) is the commonly used BJ h-tert immortalized fibroblast. The word "affected" indicates that this fibroblast has a reduced OXPHOS function of unknown origin, as described in results section.

The H1229 cell line was transfected with the plasmid pKatushka2S (K2S from now) [22] using lipofectamine 2000 reagents (Thermo Fisher Scientific) following manufacturer instructions. The efficiency was evaluated by flow cytometry and 48 h after transfection the cells were selected for one month in DMEM containing G418 0,5 mg/mL. Several clones were isolated by limit dilution and evaluated for their growing capabilities in glucose/galactose, fluorescence intensity, and transfection stability (data not shown). The K2S positive clone, with more similar properties to the parental H1299 cell line, named H1299 K2S, was used to carry out all the following experiments.

All cells were cultured routinely in DMEM, with 10% Fetal Bovine Serum (FBS) and Penicillin Streptomycin (Gibco).

2.6. Galactose and glucose growth rates

Cell growth was assayed as described previously [23]. Briefly, cell growth was assayed after growing the cells for 4 days in DMEM containing either 4.5 g/L glucose or 0.9 g/L galactose as carbon source. The cells were harvested and counted every 24 h and the growth rates were calculated using *Doubling Time Software v3.1.0* (http://www.doublingtime.com). Mean was calculated from at least three different experiments.

2.7. Co-culture experiments

Cells were co-cultivated, without refreshing the media, for 4 days. Cells reached approximately a 90% confluence and were analyzed by flow cytometry or confocal microscopy.

The experiments involving fibroblast cells were seeded at 1:3 ratio (tumor cell line: fibroblast). The day of the analysis, cell lines proportions were near 1:1 due to their diverse growth rates. For the effect between different tumor cell lines (A549 and H1299), cells were seeded accordingly to their growth rate to reach approximately a final ratio of 1:1.

To study the involvement of the basal fibroblast OXPHOS function in this process, fibroblasts were treated with 50 μg/mL of EtBr prior the experiments. After four days of drug exposure, the EtBr was removed and the fibroblasts were co-cultivated and analyzed as described above.

2.8. Flow cytometry

The mitochondrial inner membrane potential (MIMP) and Cytoplasmic ROS were assessed using tetramethyl rhodamine ester (TMRE, Invitrogen) and 2′,7′-dichlorodihydrofluorescein diacetate (H_2DCF-DA, Invitrogen) respectively.

After addition of the fluorophores (30 μM H_2DCF-DA, 100 nM TMRE) and incubation at 37 °C for 30 min in the dark, cells were collected in DMEM and analyzed immediately with a MACSQuant® (Miltenyi-Biotec) flow cytometer. Forward and side scatter were used to gate the viable population of cells and the mean fluorescence intensity was determined with FLOWJO (TreeStar). K2S or EpCAM (CD326, Miltenyi-Biotec) positivity in the 655–730 nm bandpass channel was used to distinguish between tumor and fibroblast cells in co-culture.

For cell sorting, 4×10^6 co-cultured cells were analyzed and sorted using a FASCAria II sorter in two populations (K2S positive and K2S negative) corresponding to H1299 cells or fibroblasts respectively. Monocultured cells mixed just before sorting were used as control. Cells were centrifuged after cell sorting and the pellets were immediately frozen until RNA extraction.

For the effect of TGF-β on MIMP and ROS levels, 0.75×10^6 cells were grown on MW6 plates and TGF-β was added to a final concentration of 10 ng/μL and refreshed every day. After 4 days, cells were harvested and MIMP and ROS were evaluated as described previously.

2.9. Immunofluorescence analysis

After 4 days of co-culture, immunofluorescences using specific antibodies for MCT4 (sc-50329, Santa Cruz Biotechnology), TOM20 (sc-17764, Santa Cruz Biotechnology) and α-SMA (1 A4; Abcam) were carried out as described previously [24].

2.10. Statistics

Results were analyzed using a 2-tailed Student's *t*-test to assess statistical significance. Differences in PGC-1α and GAPDH/MT-CO1 ratio levels between Low and High fibrosis groups were evaluated using ANOVA. Bivariate correlations studies between gene expressions were analyzed using the Pearson correlation test. Values of $P < 0.05$ were considered statistically significant.

3. Results and discussion

3.1. The fibroblast component increases the glycolytic phenotype of tumors

As a first approach to study the role of the fibroblast component of tumors, we studied the correlation of PGC-1α (master regulator of mitochondrial metabolism) and the GAPDH/MT-CO1 ratio mRNA levels with the fibrosis grade in a cohort of 12 stage IIIA lung adenocarcinoma patients (Fig. 1A). The results showed significant differences in PGC-1α ($p = 0.048$) and GAPDH/MT-CO1 levels ($p = 0.006$) between high and low fibrosis grade in the tumor biopsies. Interestingly, an increase in fibroblast component present in the tumor leads to higher levels of the ratio GAPDH/MT-CO1 and lower levels of PGC-1α, which are typical of an increased glycolytic metabolism and increased PET uptake [25].

To confirm these results, expression data from 73 patients with stage IIIA pulmonary adenocarcinoma present in the TCGA database were analyzed using the bioinformatic tool "R2: Genomics Analysis and Visualization Platform". The correlations between vimentin levels (as marker of the fibroblast component) with the levels of genes related to glucose metabolism (Glycolysis, TCA and OXPHOS system) were analyzed. The results show a similar change to that described in our cohort of patients (Fig. 1B and Supplementary Table 1). Overall, the results show a positive correlation of vimentin levels with genes related to an increase in glycolytic metabolism (GLUT3, HIF1A, HK3, ENO, PFKFB4…). On the other hand, genes related to the Krebs cycle (FH, MPC2, IDH3A, CS, SUCLG1…) or related to OXPHOS complexes (ATP5G3, NUDFA8,9,10, SDHA,C, COX5A…) and their assembly factors (COA5, COA6, NDUFAF5, UQCC2…) negatively correlate with vimentin levels in the tumor. Interestingly, some of these genes have been described in CAFs reprograming. The downregulation of IDH3A (Isocitrate dehydrogenase 3α) has been pointed out as responsible for the metabolic switch in CAFs trough HIF1α stabilization [26]. Remarkably, the only OXPHOS subunits that correlate positively with the vimentin levels are NDUFA4L2, COX7A1 y COX7B2, being the first two subunits related to hypoxia [27–29] and the third of unknown function.

It seems clear that an increase in fibroblast component in the tumor produces an increase in glycolytic genes with a decrease in OXPHOS genes. However, in literature, the glucose metabolism of differentiated cells such as normal fibroblasts is more oxidative than the metabolism of proliferative tumor cells [2].

Our results evaluating the metabolism of monocultured tumor cells (A549 and H1299) and normal fibroblasts confirm this. The mitochondrial inner membrane potential (MIMP) and the galactose to glucose growth ratio were higher for the fibroblast cell lines compared to the tumor cell lines A549 and H1299 (Fig. 1C).

Thus, despite the behavior of the cells in monoculture, the results on the tumor biopsies showed another role for the fibroblasts. Both results would indicate a possible effect of metabolic reprogramming towards glycolytic metabolism in the CAFs of NSCLC, that would modify the PET images [30]. However, we cannot rule out whether this relationship is produced by a specific metabolic change of tumor cells that would be more glycolytic in response to the fibroblasts present in the microenvironment, if it is the presence of metabolically reprogramed fibroblasts in the sample with a more glycolytic metabolism, or even a combination of both theories.

3.2. The in vitro co-culture of fibroblasts and NSCLC cells induce a metabolic reprogramming in both cell types

To clarify these issues and to deepen the mechanisms of this metabolic relationship in NSCLC we decided to move on to an *in vitro* model of co-cultured tumor and fibroblasts cell lines (Fig. 2A).

To identify the A549 cells in the co-culture analysis, we exploited their positivity for the epithelial membrane marker EpCAM, which efficiently discriminates these cells from the accompanying fibroblasts through antibody labeling. On the contrary, since the H1299 line has lost many of the epithelial markers it is not possible to distinguish it from the co-cultured fibroblasts. Thus, we transfected the H1299 cell line to stably express the far-red fluorescent protein Katushka2S [22]. This strategy allowed us to identify the different cell lines when co-cultured with fibroblasts and measure other parameters, both by flow cytometry and confocal microscopy (Fig. 2A).

After 4 days of co-culture with CF1 (Control Fibroblast 1), the MIMP was measured. MIMP is one of the most representative parameters modified in the metabolic reprogramming of co-cultured cells [10]. Surprisingly, we only saw changes in MIMP for the H1299 cell line, but no changes were observed for A549 cells when co-cultured (Fig. 2B). Furthermore, when CF1 was co-cultured with the H1299 cell line a decrease in the MIMP was observed, effect that does not occur when

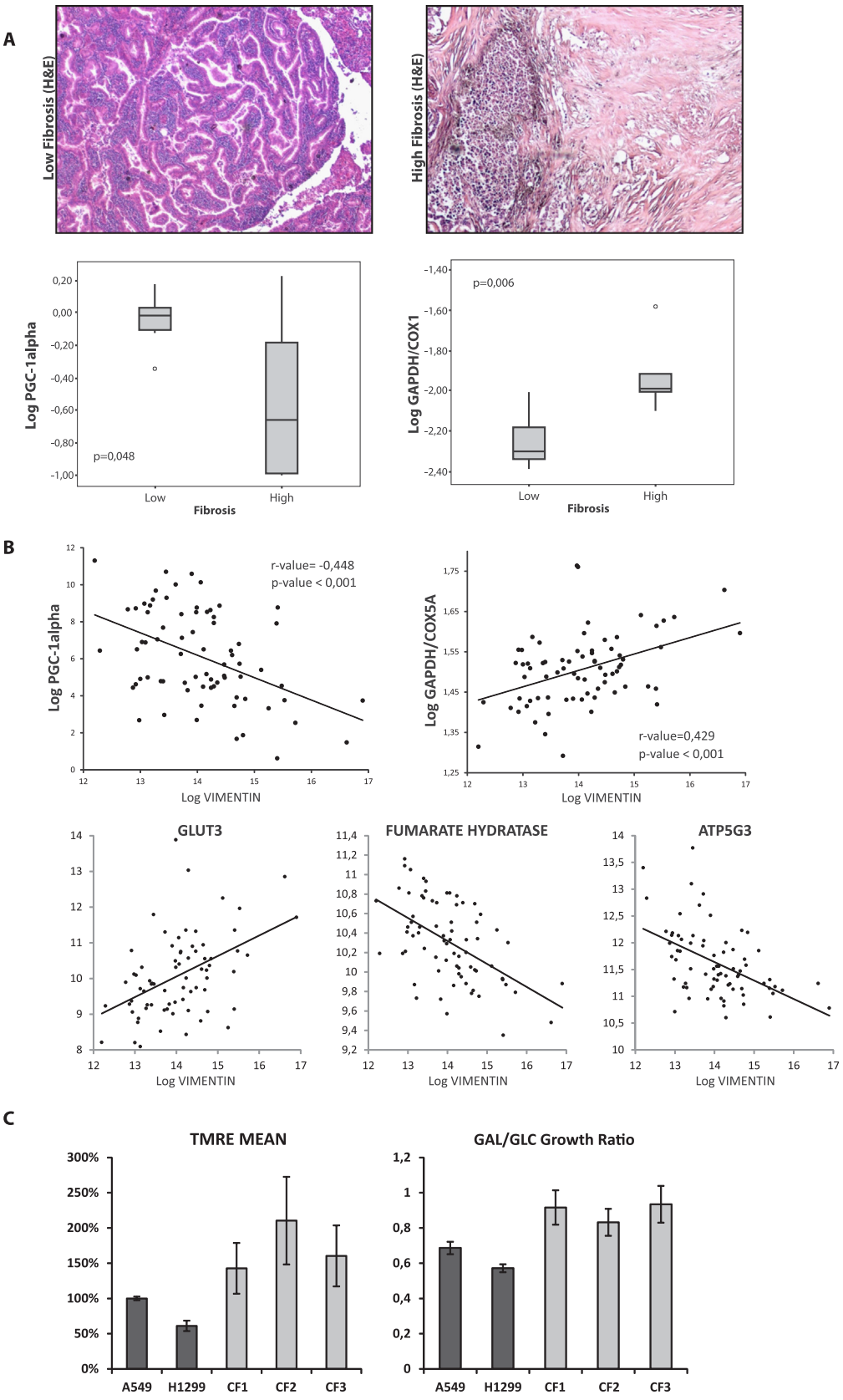

Fig. 1. The fibroblast component increases the glycolytic phenotype of tumors. (A) Upper panels, representative images for High and Low desmoplastic stroma in NSCLC samples. Lower panels, PGC-1α and GAPDH/COX1 mRNA levels correlate with fibrosis grade. (B) Representative graphs showing the correlation of vimentin expression with different glucose metabolism genes. (C) Monocultured normal fibroblasts (CF1, CF2, CF3) have higher OXPHOS function than tumor cell lines.

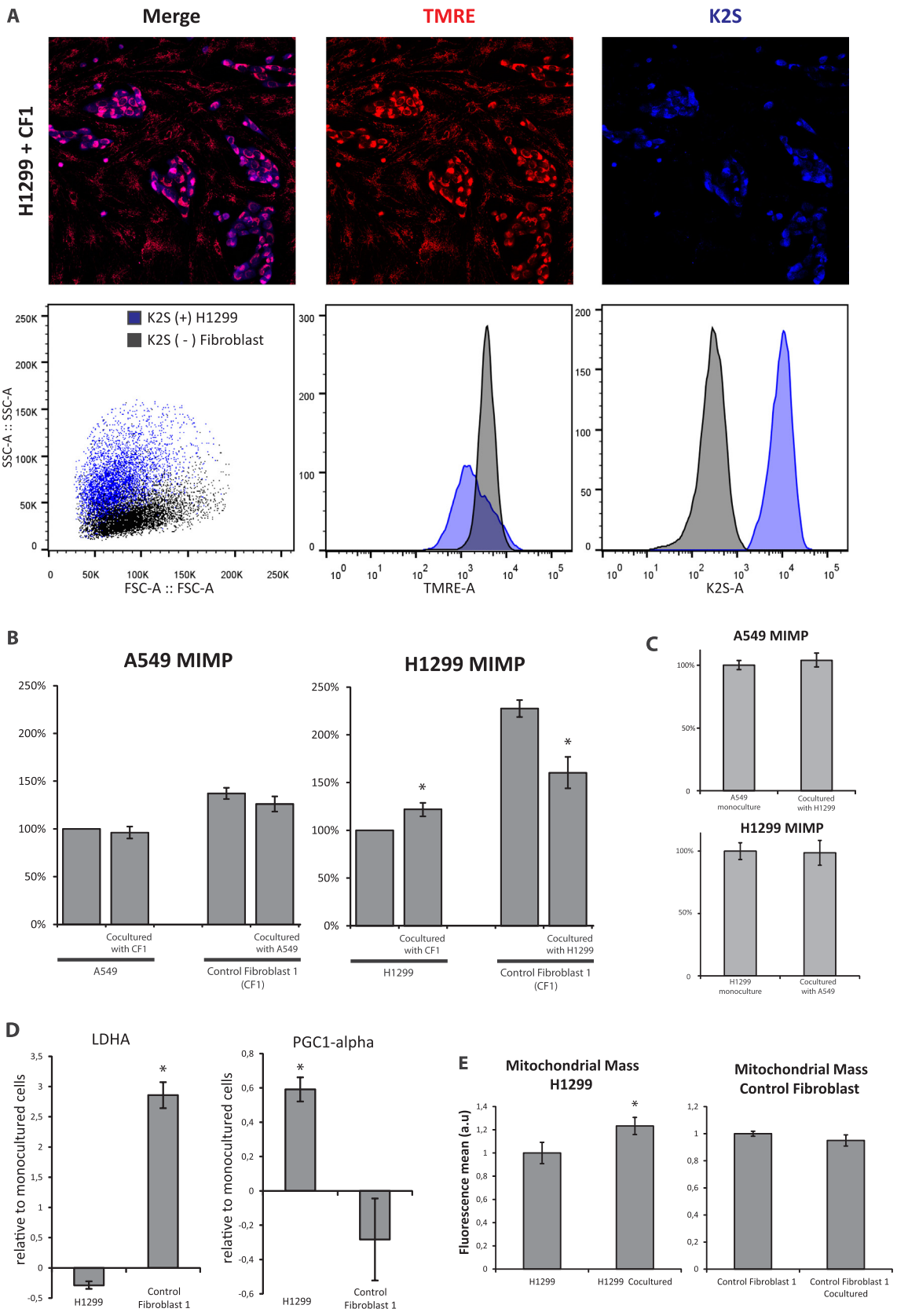

(caption on next page)

CF1 is co-cultured with the A549 cell line.

To test if this metabolic reprogramming on H1299 cells was fibroblast-specific, or if it was just produced by different cells that cohabit in the same space, we co-cultured the H1299 K2S cell line with A549 cells (Fig. 2C). The results showed no significant differences in both cell lines when co-cultured together, reinforcing the specific role of the

Fig. 2. The Effect of fibroblast co-culture in NSCLC cell lines. (A) Representative image of the co-cultures. Upper panel, confocal image of H1299 cells co-cultured with control fibroblasts (CF1). TMRE in red, H1299 K2S positive cells in blue. Lower panel, representative flow cytometry analysis of the co-cultures. Fibroblast and tumor cells were not distinguishable by size and complexity (forward and side scatter). K2S (for H1299 cells) or EpCAM (for A549 cells) positivity was used to gate and discriminate the tumor cells from the fibroblasts (B) MIMP was evaluated as TMRE fluorescence determined by flow cytometry. Data are means relative to monocultured tumor cells. Note that there are significant differences in co-cultured cells for the H1299 but not for A549 cell line. (C) No significant differences in MIMP were seen in the co-culture between tumor cell lines. (D) The effect of fibroblast co-culture on LDHA and PGC-1α mRNA levels determinated by RT-qPCR (E) Mitochondrial mass was determinated by confocal quantification of TOM20 expression. Data are means from at least three different experiments and are represented relative to monocultured cells. Error bars indicate standard deviation. Student's *t*-test p-value was considered to be statistically significant when was < 0.05 ($^* = p \leq 0.05$).

fibroblasts in this process.

We measured the LDHA and PGC-1α mRNA levels after the co-culture in both, H1299 and fibroblast cells (Fig. 2D). The results showed an increase of LDHA expression in the co-cultured fibroblasts and an increase of PGC-1α in the co-cultured tumor cells supporting a metabolic shift towards glycolysis in the fibroblasts and a metabolic shift towards OXPHOS in the tumor cells.

The OXPHOS function modification has been associated with an increase in mitochondrial mass in co-cultured tumor cells and a decrease of it in the fibroblasts [10,12]. Beyond the levels of PGC-1α, we used the amount of TOM20 protein to directly asses the mitochondrial mass by confocal microscopy independently of the MIMP. The quantification of this protein revealed a significant increase of the mitochondrial mass when the tumor cells are co-cultured with control fibroblasts, however no statistically significant differences were seen on co-cultured control fibroblasts (Fig. 2E). This point out different mechanisms for the MIMP changes in each cell type. Thus, the MIMP rise in tumor cells may be associated to PGC-1α and mitochondrial mass increase. However, the decrease of MIMP in fibroblast occurs without any significant modification in PGC-1α or mitochondrial mass levels.

These results support the existence of a metabolic reprogramming in NSCLC cells and fibroblasts *in vitro*, although this is restricted to some cell lines. Furthermore, these results may indicate that this change towards a more glycolytic metabolism in the whole tumor in patients with increased amount of fibroblasts is caused by the increased glycolytic metabolism of CAFs. This would also reinforce why fibroblasts participate in a worse prognosis of the patient [31], since they not only favor immunosuppression [32], metastasis [33] or drug resistance [7], but also would generate a tumor mass with a greater glucose uptake, which is usually associated with tumor's aggressiveness [34,35].

The fact that one tumor cell line induces this phenomenon and the other one does not on the same fibroblast cell line speaks of some determining characteristic of this process present in the tumor cell line. If these differences were also to be found in patients, it would be possible to identify different groups of patients based on their ability to induce this effect on the microenvironment, which would have implications for the diagnosis, staging or new drugs development.

3.3. Fibroblast metabolic reprogramming is not dependent on α-SMA expression

In literature, the metabolic coupling between fibroblasts and tumor cells is associated with the fibroblast activation process measured as α-SMA expression [36]. The role of α-SMA levels in NSCLC is controversial, with studies indicating that it is an unfavorable prognostic factor [37] and studies in which α-SMA did not showed any prognostic information [38].

We characterized the ability to activate fibroblasts from the two NSCLC cell lines used in the co-culture experiments (A549 and H1299). Our results show that the A549 cell line and the H1299 cell line present different ability to activate fibroblasts when co-cultured, measured as the induction of α-SMA expression in the fibroblasts (Fig. 3A). After 4 days of co-culture, A549 cells induce an increase in α-SMA expression (at both, mRNA and protein levels) in the two different fibroblast cell lines. On the other hand, H1299 cells are only capable of activate the CF1, and to a much lesser extent than A549 cells.

This differential ability of the tumor cells correlates with the expression of epithelial markers, such as EpCAM (Fig. 3B) and E-Cadherin (data not shown), as described before [39]. The H1299 cells with more mesenchymal characteristics were less effective at activating α-SMA expression than A549 cells with more epithelial characteristics.

Interestingly, since A549 is the cell line that induces more α-SMA in the fibroblasts but it is not able to reproduce the metabolic change, these results question the assumption in which the reverse Warburg effect is associated with the fibroblast activation, suggesting that these phenomena are two different entities that do not necessarily occur together.

On the other hand, these *in vitro* results suggest that α-SMA level may not be a good marker for the metabolic reprogramming effect induced by fibroblasts in NSCLC tumors. To test this hypothesis, we reanalyzed the patient's data from our cohort (data not shown) and from TCGA. The results show no correlation between α-SMA expression and PGC-1α or GAPDH/MT-CO1 (Fig. 3C).

3.4. Fibroblast basal OXPHOS function modifies tumor cells metabolic reprogramming

It seems clear that there is a metabolic change in both cell types, whereas the H1299 tumor cells increase its OXPHOS function, the fibroblasts reduce it when co-cultured. We asked ourselves if this process occurred in a similar way if we co-cultivated the tumor cell line H1299 with a fibroblast with an affected OXPHOS function.

Coincidentally, when we characterized the mitochondrial function of the fibroblasts present in the laboratory, we observed deep differences in their galactose to glucose growth rate ratios as well as in their MIMP for one fibroblast cell line (Affected Fibroblast, AF) (Fig. 4A). This result would indicate that these fibroblasts present an OXPHOS defect of unknown origin. Interestingly, this OXPHOS defect is somehow compensated by an increased glycolytic function as evidenced by their increased LDHA mRNA levels. Moreover, in order to have an isogenic model with a decreased OXPHOS function, we treated the CF1 with EtBr (ethidium bromide) [40]. The treatment with EtBr greatly reduced the MIMP, and specifically stopped the growth of cells in galactose, without affecting their growth in glucose (Fig. 4A).

We studied the levels of MCT4 (responsible for the lactate export from the cytoplasm to the microenvironment) for both, monoculture and co-culture conditions (Fig. 4B). The basal MCT4 levels of CF1 were not detectable by immunofluorescence. On the contrary, the CF1 treated with EtBr or the Affected Fibroblast showed a notable MCT4 expression reinforcing their higher glycolytic activity. Remarkably, after the co-culture with tumor cells, an increase of MCT4 levels was induced on CF1, similarly to the LDHA increase observed (Fig. 2B) and therefore supporting a glycolytic shift in the fibroblasts. On the other hand, the CF1 treated with EtBr or the AF maintain their already high MCT4 levels that did not significantly change. Similar results were obtained analyzing MCT4 mRNA levels. CF1 showed lower MCT4 mRNA levels than the AF. Furthermore, MCT4 mRNA levels were induced in CF1 after tumor co-culture but no differences were observed after tumor co-culture in Affected Fibroblast MCT4 mRNA levels.

Additionally, after 4 days of co-culture with the different fibroblasts, the results showed a greater MIMP increase for the H1299 cell line when it is co-cultivated with fibroblasts with a diminished OXPHOS

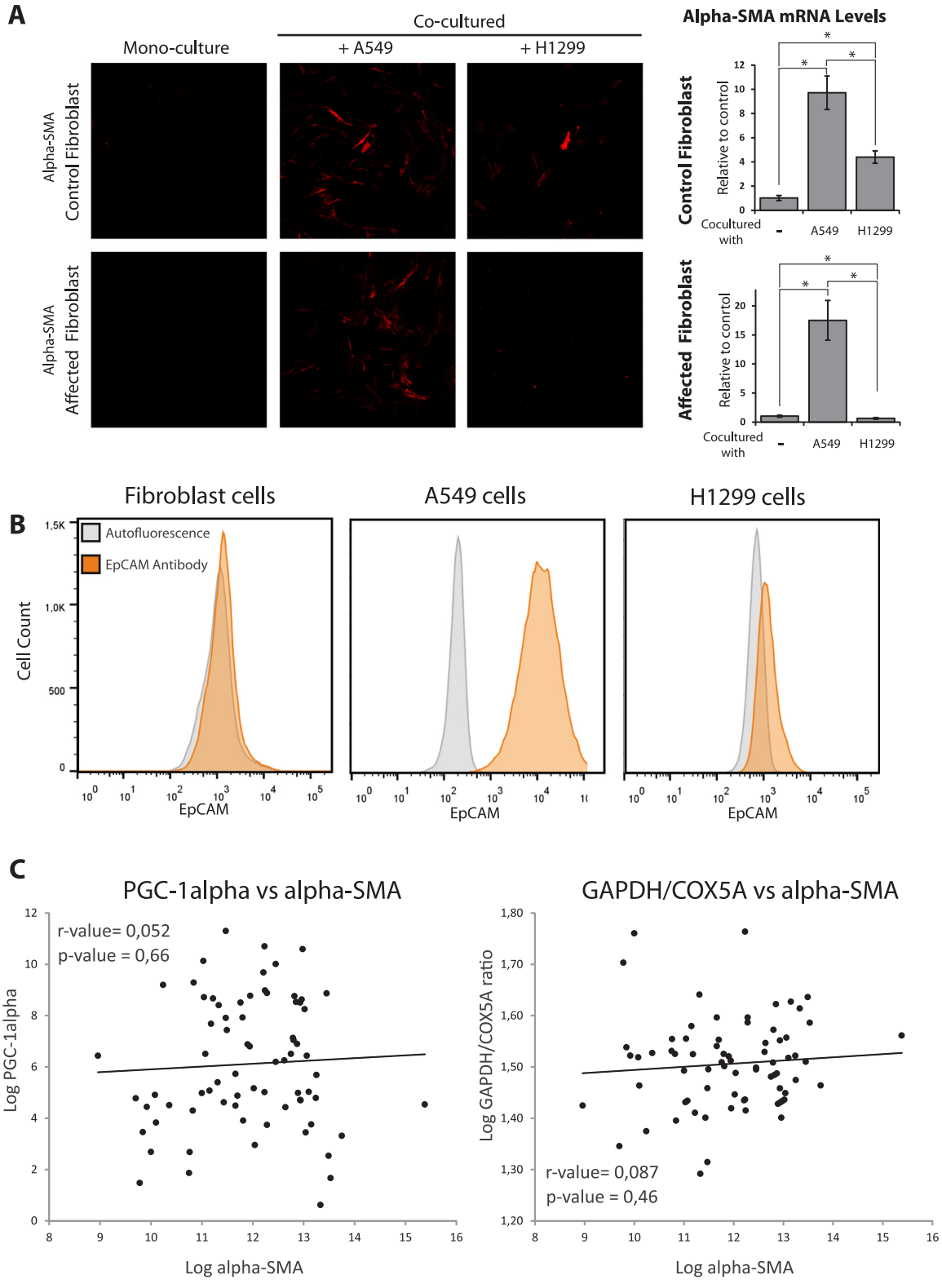

Fig. 3. Metabolic reprogramming is not dependent on α-SMA expression. (A) Left panel, α-SMA confocal images of two different fibroblasts cell lines co-cultured with A549 or H1299 tumor cells. Right panel, fibroblast α-SMA mRNA levels induced by tumor cell co-culture. Data are means from at least three different experiments. Error bars indicate standard deviation. Student's *t*-test p-value was considered to be statistically significant when was < 0.05 (* = $p \leq 0.05$). Cells in monoculture were used as controls. Note that the co-culture with A549 cells induce a higher α-SMA expression than H1299 co-culture (B) Epithelial marker EpCAM by flow cytometry. A549 cells are positive for EpCAM and E-Cadherin (data not shown) markers, on the other hand fibroblasts and H1299 cells are negative. (C) α-SMA expression do not correlate with PGC-1α or GAPDH/COX5A in patients.

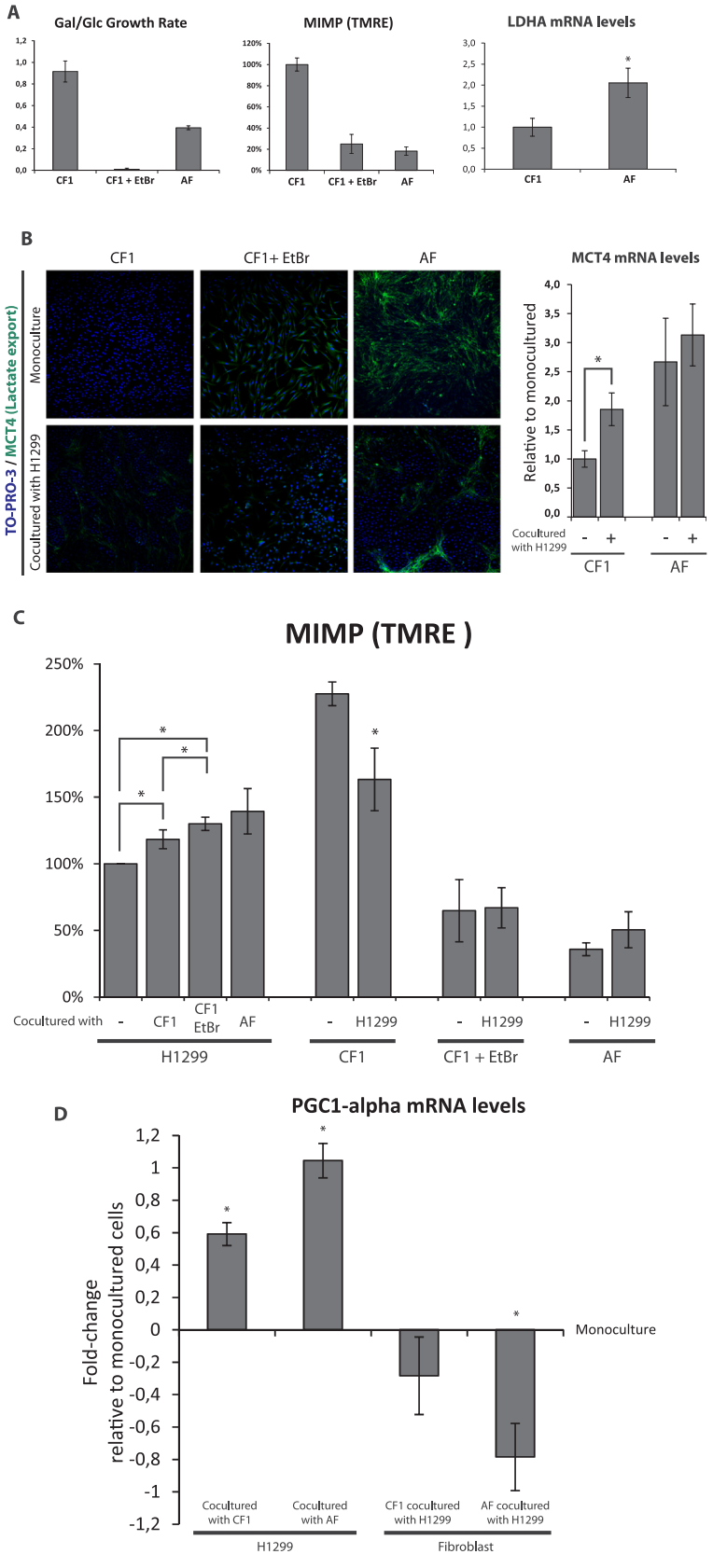

Fig. 4. The role of Fibroblast OXPHOS function in metabolic reprogramming of co-cultured cells. (A) OXPHOS function characterization of fibroblast cell lines. (CF1; Control Fibroblast 1, CF1 +EtBr; Control Fibroblast 1 + Ethidium Bromide, AF; Affected Fibroblast). Note the profound differences both in their galactose to glucose growth rate ratios as well as in their MIMP and LDHA mRNA levels. (B) Left panel, immunofluorescence confocal images of MCT4 induction in fibroblasts after 4-day co-culture with H1299 cells. (MCT4 antibody in green and TO-PRO-3 staining the nucleus in blue). Right panel, MCT4 mRNA levels induced by co-culture with H1299 cells (C) MIMP changes produced by co-culture with different fibroblast. (D) PGC-1α mRNA levels on H1299 cell line when co-cultured with control and Affected Fibroblasts and on both fibroblasts co-cultured with H1299 cell line. Data are means from at least three different experiments. Error bars indicate standard deviation. Student's *t*-test p-value was considered to be statistically significant when was < 0.05 ($*=p \leq 0.05$).

function (Fig. 4C). On the other hand, the AF and the CF1 treated with EtBr do not behave the same way as the CF1 when co-cultured with H1299. Whereas the CF1 decrease its MIMP the AF or the CF1 treated with EtBr did not show any statistical differences (Fig. 4C). It is possible that the latter cell lines are not able to diminish their OXPHOS function more than it is already reduced, which would also explain why they do not increase their expression of MCT4.

Moreover, we measured PGC-1α mRNA levels as indirect

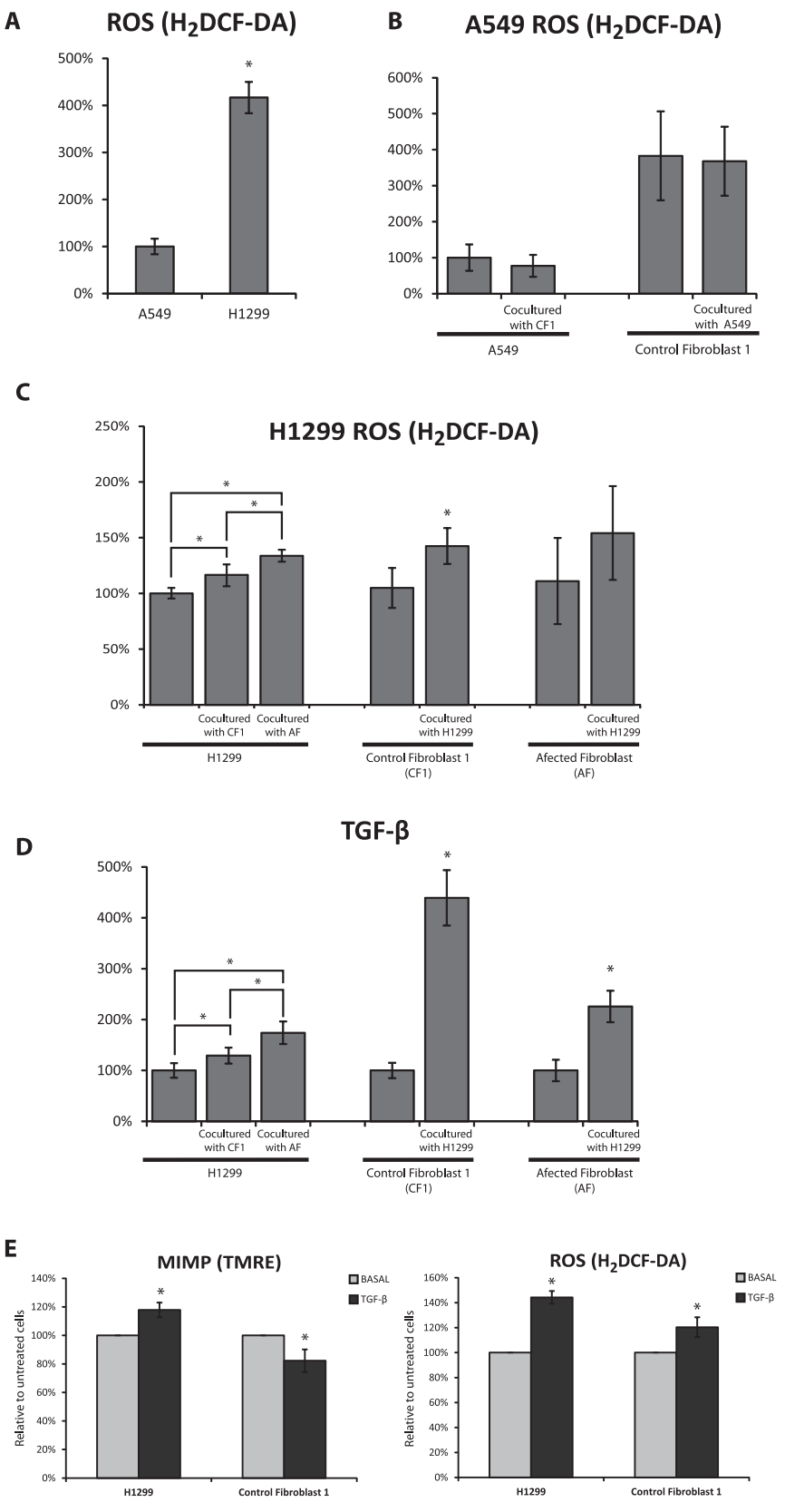

Fig. 5. Reactive Oxygen Species and TGF-β in metabolic reprogramming. ROS levels were evaluated using the H_2DCFH-DA fluorescent probe by flow cytometry. (A) Basal ROS levels in monocultured A549 and H1299 cells. Note the fourfold increase in ROS levels for the H1299 cells (B) ROS levels on A549 cells and control fibroblasts, ROS levels are not modified after co-culture. (C) H1299 cells increase their ROS levels after co-culture with two different fibroblasts cell lines. (D) TGF-β mRNA levels measured by RT-qPCR in the cells were increased in all the cell lines studied. Note that the co-culture with affected fibroblasts augments the effect on H1299 cells compared to control fibroblasts. (E) Effect on MIMP and ROS levels of TGF-β addition to monocultured cells. Data are means relative to monocultured tumor cells from at least three different experiments. Error bars indicate standard deviation. Student's *t*-test p-value was considered to be statistically significant when was < 0.05 ($* = p \leq 0.05$).

measurement of the mitochondrial biogenesis, which, as we had seen previously, was altered by the co-culture with CF1. Our results show a greater increase of the mitochondrial biogenesis when the H1299 line is co-cultivated with the AF. In turn, the decrease of PGC-1α expression is higher for these fibroblasts than for the CF1 when co-cultured with H1299 (Fig. 4D). These results would indicate that this process occurs even on an OXPHOS-affected fibroblast. In fact, this seems to facilitate the MIMP and PGC-1α increase of the tumor cells.

Fibroblasts with an affected OXPHOS function seems to facilitate the reverse Warburg effect probably through their higher supply of lactate due to their impaired OXPHOS function [41]. Recently, lactate has been proposed as a potential carbon source for lung tumors *in vivo* [42] and metabolic differences between CAFs from high and low glycolytic tumors have been found [34].

All this data combined with the variability of mitochondrial function among healthy individuals (a common drawback in the study of mitochondrial diseases [43]) would place the OXPHOS performance of fibroblasts as a modifier element of tumor metabolism.

In relation to the previous sections, these results confirm that the H1299 cell line presents the ability to modify the metabolic microenvironment in which is present, since it occurs in the presence of two fibroblasts from different origins. Furthermore, since the AF do not become significantly activated in the presence of the H1299 cell line (Fig. 3A), but nevertheless they produce a greater effect on the MIMP of the tumor line, this result confirms that this process of metabolic reprogramming is independent of fibroblast activation measured as α-SMA induction.

3.5. Reactive oxygen species levels in co-cultured NSCLC cells

One of the main factors responsible for metabolism reprogramming is ROS [10]. We measured the basal ROS, in both tumor cell lines, using the fluorescent probe H_2DCFH-DA. The results showed a significant fourfold increase of ROS for H1299 cells compared to A549 cells (Fig. 5A).

When we analyzed the levels of ROS in the co-cultures, we observed a change of them for H1299 cells, but not for A549 cells, that maintain the same ROS levels (Fig. 5B-C). Interestingly in H1299 co-culture, ROS levels increase in both cell types, suggesting some kind of reciprocal signal.

In addition, as well as for membrane potential, there is a differential effect of the co-culture with different fibroblast cells for ROS. The co-culture with the AF produces a greater increase of ROS in the tumor cells than the co-culture with CF1. On the contrary, the increase of ROS in both fibroblasts was similar.

The differences in basal ROS levels between tumor cells might explain why this metabolic reprogramming is restricted to the H1299 cells, while A549 cells are not capable of producing this effect. Reinforcing our results, the role of ROS in this phenomenon has been pointed out previously as the starting mechanism for this process [10].

On the other hand, it has been described how an increase of ROS in the cell media produces an increase of the fibroblast TGF-β levels [44]. Our results showed an increase of TGF-β mRNA levels for all the cell lines when co-cultured (Fig. 5D). Again, the effect on the tumor cell line is greater when it is co-cultured with the AF. In turn TGF-β levels are key in the metabolic reprogramming towards an increase of fibroblast glycolysis and production of lactic acid, substrate for the tumor cells [26,36]. When we incubate the cells with TGF-β we see a similar effect to that produced by the co-culture; tumor cells increase the MIMP while fibroblasts reduce it. On the other hand TGF-β induces an increase of ROS in the two cell lines similar to that induced by the co-culture (Fig. 5E).

4. Conclusions

This study provides a better understanding of the actual tumor metabolism as it focuses on functional studies and takes into account that tumor cells are not isolated but are in constant communication to other cell types forming a particular microenvironment. Our results support the existence of the Reverse Warburg Effect in lung cancer. Interestingly, this process is restrained to some tumor cell lines; it is not necessarily associated to fibroblast activation; may be modified by different fibroblasts and implies an alteration of ROS and TGF-β levels.

Out of all the previously stated information, knowing the metabolic relationships between different cell types may provide: improvements in diagnosis through better interpretation of PET images; identification of different groups of patients according to their metabolic microenvironment that could have different prognoses; or even the discovery of key therapeutic targets for developing new drugs.

Conflict of interest

The authors declare no conflicts of interest.

Funding

Work in the authors' laboratories is supported by "Instituto de Salud Carlos III" PI13/01806 and PIE14/0064 to M.P. A.C-B, received a Spanish Lung Cancer Group fellowship. R.L-B, is supported by Comunidad Autónoma de Madrid "Garantía juvenil" contract.

Appendix A. Supplementary material

Supplementary data associated with this article can be found in the online version at doi:10.1016/j.freeradbiomed.2018.10.450.

References

[1] D. Hanahan, R.A. Weinberg, Hallmarks of cancer: the next generation, Cell 144 (2011) 646–674, https://doi.org/10.1016/j.cell.2011.02.013S0092-8674(11)00127-9.
[2] M.G. Vander Heiden, L.C. Cantley, C.B. Thompson, Understanding the Warburg effect: the metabolic requirements of cell proliferation, Sci. (80-.) 324 (2009) 1029–1033, https://doi.org/10.1126/science.1160809324/5930/1029.
[3] P.S. Ward, C.B. Thompson, Metabolic Reprogramming: a Cancer Hallmark Even Warburg Did Not Anticipate, Cancer Cell. 21 (2012) 297–308, https://doi.org/10.1016/j.ccr.2012.02.014.
[4] R.L. Wahl, R.L. Cody, G.D. Hutchins, E.E. Mudgett, Primary and metastatic breast carcinoma: initial clinical evaluation with PET with the radiolabeled glucose analogue 2-[F-18]-fluoro-2-deoxy-D-glucose, Radiology 179 (1991) 765–770, https://doi.org/10.1148/radiology.179.3.2027989.
[5] S. Pavlides, D. Whitaker-Menezes, R. Castello-Cros, N. Flomenberg, A.K. Witkiewicz, P.G. Frank, et al., The reverse Warburg effect: aerobic glycolysis in cancer associated fibroblasts and the tumor stroma, Cell Cycle 8 (2009) 3984–4001, https://doi.org/10.4161/cc.8.23.10238.
[6] A. Orimo, P.B. Gupta, D.C. Sgroi, F. Arenzana-Seisdedos, T. Delaunay, R. Naeem, et al., Stromal fibroblasts present in invasive human breast carcinomas promote tumor growth and angiogenesis through elevated SDF-1/CXCL12 secretion, Cell 121 (2005) 335–348, https://doi.org/10.1016/j.cell.2005.02.034.
[7] W. Wang, I. Kryczek, J.R. Liu, W. Zou, H. Lin, L. Tan, et al., Effector T Cells Abrogate Stroma-Mediated Chemoresistance in Ovarian Cancer, Cell (2016) 1–14, https://doi.org/10.1016/j.cell.2016.04.009.
[8] R. Kalluri, The biology and function of fibroblasts in cancer, Nat. Publ. Gr. 16 (2016) 582–598, https://doi.org/10.1038/nrc.2016.73.
[9] M. Kraman, P.J. Bambrough, J.N. Arnold, E.W. Roberts, L. Magiera, J.O. Jones, et al., Suppression of antitumor immunity by stromal cells expressing fibroblast activation protein-alpha, Science 330 (2010) 827–830, https://doi.org/10.1126/science.1195300.
[10] U.E. Martinez-Outschoorn, Z. Lin, C. Trimmer, N. Flomenberg, C. Wang, S. Pavlides, et al., Cancer cells metabolically "fertilize" the tumor microenvironment with hydrogen peroxide, driving the Warburg effect: implications for PET imaging of human tumors, Cell Cycle 10 (2011) 2504–2520, https://doi.org/10.4161/cc.10.15.16585.
[11] D. Whitaker-Menezes, U.E. Martinez-Outschoorn, N. Flomenberg, R. Birbe, A.K. Witkiewicz, A. Howell, et al., Hyperactivation of oxidative mitochondrial metabolism in epithelial cancer cells in situ, Cell Cycle 10 (2011) 4047–4064, https://doi.org/10.4161/cc.10.23.18151.
[12] A.F. Salem, D. Whitaker-Menezes, Z. Lin, U.E. Martinez-Outschoorn, H.B. Tanowitz, M.S. Al-Zoubi, et al., Two-compartment tumor metabolism: autophagy in the tumor microenvironment and oxidative mitochondrial metabolism (OXPHOS) in cancer cells, Cell Cycle 11 (2012) 2545–2556, https://doi.org/10.4161/cc.20920.
[13] T. Fiaschi, A. Marini, E. Giannoni, M.L. Taddei, P. Gandellini, A. De Donatis, et al., Reciprocal metabolic reprogramming through lactate shuttle coordinately influences tumor-stroma interplay, Cancer Res. 72 (2012) 5130–5140, https://doi.org/10.1158/0008-5472.CAN-12-1949.
[14] C. Swanton, R. Govindan, Clinical Implications of Genomic Discoveries in Lung Cancer, N. Engl. J. Med. 374 (2016) 1864–1873, https://doi.org/10.1056/NEJMra1504688.
[15] Z. Chen, C.M. Fillmore, P.S. Hammerman, C.F. Kim, K.-K. Wong, Non-small-cell lung cancers: a heterogeneous set of diseases, Nat. Rev. Cancer 14 (2014) 535–546, https://doi.org/10.1038/nrc3775.
[16] M. Reck, D.F. Heigener, T. Mok, J.-C. Soria, K.F. Rabe, Management of non-small-

cell lung cancer: recent developments, Lancet 382 (2013) 709–719, https://doi.org/10.1016/S0140-6736(13)61502-0.
[17] S. Novello, F. Barlesi, R. Califano, T. Cufer, S. Ekman, M.G. Levra, et al., Metastatic non-small-cell lung cancer: ESMO Clinical Practice Guidelines for diagnosis, treatment and follow-up, Ann. Oncol. 27 (2016) V1–V27, https://doi.org/10.1093/annonc/mdw326.
[18] R.M. Bremnes, T. Dønnem, S. Al-Saad, K. Al-Shibli, S. Andersen, R. Sirera, et al., The role of tumor stroma in cancer progression and prognosis: emphasis on carcinoma-associated fibroblasts and non-small cell lung cancer, J. Thorac. Oncol. 6 (2011) 209–217, https://doi.org/10.1097/JTO.0b013e3181f8a1bd.
[19] K. Kaira, M. Serizawa, Y. Koh, T. Takahashi, A. Yamaguchi, H. Hanaoka, et al., Biological significance of 18F-FDG uptake on PET in patients with non-small-cell lung cancer, Lung Cancer 83 (2014) 197–204, https://doi.org/10.1016/j.lungcan.2013.11.025.
[20] R.M. Bremnes, T. Dønnem, S. Al-Saad, K. Al-Shibli, S. Andersen, R. Sirera, et al., The role of tumor stroma in cancer progression and prognosis, J. Thorac. Oncol. 6 (2011) 209–217, https://doi.org/10.1097/JTO.0b013e3181f8a1bd.
[21] S. Søes, B.S. Sørensen, J. Alsner, J. Overgaard, H. Hager, L.L. Hansen, et al., Identification of accurate reference genes for RT-qPCR analysis of formalin-fixed paraffin-embedded tissue from primary non-small cell lung cancers and brain and lymph node metastases, Lung Cancer 81 (2013) 180–186, https://doi.org/10.1016/j.lungcan.2013.04.007.
[22] K.E. Luker, P. Pata, I.I. Shemiakina, A. Pereverzeva, a.C. Stacer, D.S. Shcherbo, et al., Comparative study reveals better far-red fluorescent protein for whole body imaging, Sci. Rep. 5 (2015) 10332, https://doi.org/10.1038/srep10332.
[23] A. Cruz-Bermúdez, C.G. Vallejo, R.J. Vicente-Blanco, M.E. Gallardo, M.Á. Fernández-Moreno, M. Quintanilla, et al., Enhanced tumorigenicity by mitochondrial DNA mild mutations, Oncotarget 6 (2015) 13628–13643, https://doi.org/10.18632/oncotarget.3698.
[24] E. Martínez-martínez, A. Martín-ruiz, P. Martín, M. Provencio, J.M. García, CB 2 cannabinoid receptor activation promotes colon cancer progression via AKT / GSK3β signaling pathway, 7, 2016.
[25] A. Cruz-Bermúdez, R.J. Vicente-Blanco, R. Laza-Briviesca, A. García-Grande, S. Laine-Menéndez, L. Gutiérrez, et al., PGC-1alpha levels correlate with survival in patients with stage III NSCLC and may define a new biomarker to metabolism-targeted therapy, Sci. Rep. (2017), https://doi.org/10.1038/s41598-017-17009-6.
[26] D. Zhang, Y. Wang, Z. Shi, J. Liu, P. Sun, X. Hou, et al., Metabolic reprogramming of cancer-associated fibroblasts by IDH3α downregulation, Cell Rep. 10 (2015) 1335–1348, https://doi.org/10.1016/j.celrep.2015.02.006.
[27] D. Tello, E. Balsa, B. Acosta-Iborra, E. Fuertes-Yebra, A. Elorza, Á. Ordóñez, et al., Induction of the mitochondrial NDUFA4L2 protein by HIF-1α decreases oxygen consumption by inhibiting Complex I activity, Cell Metab. 14 (2011) 768–779, https://doi.org/10.1016/j.cmet.2011.10.008.
[28] H.J. Hwang, S.G. Lynn, A. Vengellur, Y. Saini, A. Grier, S.M. Ferguson-miller, et al., Hypoxia Inducible Factors (HIFs) modulate mitochondrial oxygen consumption and transcriptional regulation of nuclear encoded electron transport chain genes. 〈https://doi.org/10.1021/bi5012892〉, 2015.
[29] A. Cruz-Bermúdez, R.J. Vicente-Blanco, E. Gonzalez-Vioque, M. Provencio, M.Á. Fernández-Moreno, R. Garesse, Spotlight on the relevance of mtDNA in cancer, Clin. Transl. Oncol. (2016) 1–10, https://doi.org/10.1007/s12094-016-1561-6.
[30] G. Zhang, J. Li, X. Wang, Y. Ma, X. Yin, F. Wang, et al., The reverse warburg effect and 18F-FDG uptake in non-small cell lung cancer A549 in Mice: a pilot study, J. Nucl. Med. 56 (2015) 607–612, https://doi.org/10.2967/jnumed.114.148254.
[31] R. Navab, D. Strumpf, B. Bandarchi, C. Zhu, M. Pintilie, V. Rohan, Prognostic gene-expression signature of carcinoma- associated fi broblasts in non-small cell lung cancer, Proc. Natl. Acad. Sci. USA 108 (2011) 7160–7165, https://doi.org/10.1073/pnas.1014506108/-/DCSupplemental.www.pnas.org/cgi//10.1073/pnas.1014506108.
[32] A. Costa, Y. Kieffer, A. Scholer-Dahirel, F. Pelon, B. Bourachot, M. Cardon, et al., Fibroblast heterogeneity and immunosuppressive environment in human breast cancer (e10), Cancer Cell. 33 (2018) 463–479, https://doi.org/10.1016/j.ccell.2018.01.011.
[33] L. Wang, L. Cao, H. Wang, B. Liu, Q. Zhang, Z. Meng, et al., Cancer-associated fibroblasts enhance metastatic potential of lung cancer cells through IL-6/STAT3 signaling pathway, Oncotarget 8 (2017) 76116–76128, https://doi.org/10.18632/oncotarget.18814.
[34] V.K. Chaudhri, G.G. Salzler, S. a. Dick, M.S. Buckman, R. Sordella, E.D. Karoly, et al., Metabolic alterations in lung cancer-associated fibroblasts correlated with increased glycolytic metabolism of the tumor, Mol. Cancer Res. 11 (2013) 579–592, https://doi.org/10.1158/1541-7786.MCR-12-0437-T.
[35] J. Liu, M. Dong, X. Sun, W. Li, L. Xing, J. Yu, Prognostic value of18F-FDG PET/CT in surgical non-small cell lung cancer: a meta-analysis, PLoS One 11 (2016) 1–19, https://doi.org/10.1371/journal.pone.0146195.
[36] C. Guido, D. Whitaker-menezes, C. Capparelli, R. Balliet, Z. Lin, R.G. Pestell, et al., Metabolic reprogramming of cancer-associated fibroblasts by TGF- β drives tumor growth Connecting TGF- β signaling with " Warburg-like" cancer metabolism and L-lactate production, Cell Cycle 11 (2012) 3019–3035.
[37] Y. Chen, L. Zou, Y. Zhang, Y. Chen, P. Xing, W. Yang, et al., Transforming growth factor-B1 and a-smooth muscle actin in stromal fibroblasts are associated with a poor prognosis in patients with clinical stage I-IIIA nonsmall cell lung cancer after curative resection, Tumor Biol. 35 (2014) 6707–6713, https://doi.org/10.1007/s13277-014-1908-y.
[38] T.K. Kilvaer, M.R. Khanehkenari, T. Hellevik, S. Al-saad, Cancer Associated Fibroblasts in Stage I-IIIA NSCLC: Prognostic Impact and Their Correlations with Tumor Molecular Markers 1–15. doi: 10.1371/journal.pone.0134965, 2015.
[39] C. Eberlein, C. Rooney, S.J. Ross, M. Farren, H.M. Weir, S.T. Barry, E-Cadherin and EpCAM expression by NSCLC tumour cells associate with normal fibroblast activation through a pathway initiated by integrin αvβ6 and maintained through TGFβ signalling, Oncogene 34 (2014) 1–13, https://doi.org/10.1038/onc.2013.600.
[40] L.P. Kao, D. Ovchinnikov, E. Wolvetang, The effect of ethidium bromide and chloramphenicol on mitochondrial biogenesis in primary human fibroblasts, Toxicol. Appl. Pharmacol. 261 (2012) 42–49, https://doi.org/10.1016/j.taap.2012.03.009.
[41] R.M. Balliet, C. Capparelli, C. Guido, T.G. Pestell, U.E. Martinez-outschoorn, Z. Lin, et al., Mitochondrial oxidative stress in cancer-associated fibroblasts drives lactate production, promoting breast cancer tumor growth Understanding the aging and cancer connection 4065–4073, 2011.
[42] C.T. Hensley, B. Faubert, Q. Yuan, N. Lev-Cohain, E. Jin, J. Kim, et al., Metabolic heterogeneity in human lung tumors, Cell 164 (2016) 681–694, https://doi.org/10.1016/j.cell.2015.12.034.
[43] A. Cruz-Bermúdez, R.J. Vicente-Blanco, R. Hernández-Sierra, M. Montero, J. Alvarez, M. González Manrique, et al., Functional characterization of three concomitant MtDNA LHON mutations shows no synergistic effect on mitochondrial activity, PLoS One 11 (2016) e0146816, https://doi.org/10.1371/journal.pone.0146816.
[44] M. González-Ramos, I. Mora, S. De Frutos, R. Garesse, M. Rodríguez-Puyol, G. Olmos, et al., Intracellular redox equilibrium is essential for the constitutive expression of AP-1 dependent genes in resting cells: studies on TGF-β1 regulation, Int. J. Biochem. Cell Biol. 44 (2012) 963–971, https://doi.org/10.1016/j.biocel.2012.03.003.